R. & M. No. 3410

MINISTRY OF AVIATION

AERONAUTICAL RESEARCH COUNCIL
REPORTS AND MEMORANDA

Some Exploratory Measurements of Leading-Edge Vortex Positions on a Delta Wing Oscillating in Heave

By R. L. MALTBY, P. B. ENGLER and R. F. A. KEATING
with an Addendum by G. F. Moss

LONDON: HER MAJESTY'S STATIONERY OFFICE
1965
PRICE 12*s.* 6*d.* NET

Some Exploratory Measurements of Leading-Edge Vortex Positions on a Delta Wing Oscillating in Heave

By R. L. Maltby, P. B. Engler and R. F. A. Keating
with an Addendum by G. F. Moss

Communicated by the Deputy Controller Aircraft (Research and Development), Ministry of Aviation

*Reports and Memoranda No. 3410**

July, 1963

Summary.

Some measurements of vortex-core height for a heaving delta wing at high incidence are presented. A method of flow visualization using smoke was specially developed for this investigation, and a simple theory for the appearance of the smoke display is included in the text.

In the original analysis, given in the main body of the report, a phase lag of 60° was found between the height of the vortex core and the heaving motion at a frequency parameter of 3·4. In a subsequent re-analysis of the data, given as an addendum to the main text, a more detailed comparison with theory is shown along with the results of extra measurements made with pressure transducers.

LIST OF CONTENTS

* Replaces R.A.E. Tech. Note No. Aero. 2903—A.R.C. 25 269.

LIST OF CONTENTS—*continued*

LIST OF ILLUSTRATIONS

---

1. *Introduction.*

The structure of the separated flow above a highly swept delta wing at incidence has been the subject of a large number of theoretical and experimental studies but the work has been concerned mainly with steady motion. Current interest in the stability and flutter derivatives of oscillating slender wings has drawn attention to the scant knowledge of the behaviour of separated flow in these conditions although methods of estimating many of the derivatives are available[1].

A full survey of an oscillating flow field of such a complex nature would be a formidable undertaking but the possibility of obtaining a limited amount of information by flow visualization is investigated here as a means of providing some background to possible fundamental theoretical work.

The normal difficulty with smoke flow-visualization methods is that they require low wind speeds due to rapid diffusion of the smoke filaments in turbulent conditions and reliable quantitative results are only possible at unrepresentative Reynolds numbers. Condensation of water vapour near the cores of the vortices on a slender wing at high incidence and velocity has been observed[2] to provide an excellent indication of the vortex paths. To obtain similar effects over a larger range of conditions, the current investigation has included the development of a method of introducing smoke into the core at Reynolds numbers in the region of 6×10^6 based on root chord.

The sensitivity of the method was first tested in steady conditions and subsequently measurements were made of the vortex paths during heaving oscillations.

These experiments were made in the 13 ft × 9 ft Low-Speed Tunnel at the Royal Aircraft Establishment, Bedford, during November, 1961.

2. *The Smoke Generator.*

The conditions of test required a sufficient volume of smoke to be injected into the air stream over a limited area for it to be visible near the core of the leading-edge vortex at wind speeds in the region of 170 ft/sec. It was desirable that the rate of smoke delivery should be easily controllable over a period sufficient to make the necessary measurements. These conditions ruled out the possibility of generating the smoke close to the point of injection and an apparatus had to be designed which would generate the smoke outside the wind tunnel and convey it to the model through about 10 ft of tubing.

The usual types of smoke suitable for use in a wind tunnel tend to clog long supply pipes or condense on the pipe walls, and the resulting delivery is insufficient or erratic. For instance, smoke from a conventional kerosene smoke generator was found to be of very poor quality after passing through a length of $\frac{1}{2}$ inch diameter copper pipe, even when the pipe was kept hot by electrical heating tape wrapped along its entire length. Some attention was given to the smokes produced by smouldering materials like tobacco but in general they produced too much tarry matter to be acceptable. It was found, however, that in certain conditions smouldering paper produced a dense smoke which would survive passage through a cold tube without a serious amount of tarry matter being carried with it. The best results were obtained with rolls of paper towelling.

It should be noted, however, that the products of slow combustion of cellulose materials contain appreciable quantities of carbon monoxide. If this smoke has to be used in an enclosed space it is most important to keep a check on the carbon-monoxide contamination of the atmosphere. Some notes on the risk of carbon-monoxide poisoning are given in Appendix I.

A suitable smoke generator known as To.P.S.I. (Toilet Paper Smoke Installation) was designed and is illustrated in Fig. 2. It consists of two substantial steel cylinders both 12 inches high, namely the combustion chamber (12 inch diameter), and the separator (8 inch diameter) which removes the less volatile products of combustion. Both cylinders are fitted with lids which are bolted down firmly to make a good seal.

The combustion chamber is fitted with an air-supply pipe at the bottom and also a plug through which the paper is ignited. Inside this chamber, the air-supply pipe is divided into three smaller pipes arranged to distribute the incoming air. The separator is connected to the combustion chamber

by a $1\frac{1}{4}$ inch diameter pipe which is easily accessible for cleaning. The smoke-supply pipe to the wind tunnel is connected to the top of the separator by a length of gas-tight flexible metal tubing.

It appeared to be important to keep the temperature of combustion low in order to minimize the amount of tar produced and to extend the duration of smoke production. The correct burning rate was achieved by making the paper slightly damp (not wet) before loading. About $2\frac{1}{2}$ lb of paper packed loosely into the combustion chamber can be made to provide smoke for about 40 minutes.

3. *Description of Model and Tests.*

The model used is illustrated in Fig. 1. It consists of a delta plate of unit aspect ratio with a flat top and bevelled under-surface to give sharp edges all round. The model was mounted on the longitudinal centre line of the tunnel on two struts which could be reciprocated to impart a simple harmonic heaving motion to the wing with an amplitude of 1/24th of its root chord. Static force tests on this model have been reported previously in Ref. 3 (where it is referred to as Wing 8) and the lift curve is redrawn here in Fig. 4. It should be noted that, having a flat upper surface, the wing has a slight negative camber and the behaviour of the separations in the neighbourhood of zero lift is not clear.

It was found that, if the exit of the smoke pipe was correctly positioned relative to the nose of the model, the smoke was drawn into the vortex and held in the form of a tube around the vortex core. Since the bulk of the smoke is held in the votex there is little diffusion and it remained clearly visible up to a speed of 170 ft/sec. This limit was imposed by model strength and there seems little doubt that much higher speeds could otherwise have been tolerated. The position of the smoke pipe relative to the wing and the general appearance of the smoke tube are shown in Fig. 3.

Flash photographs of the smoke trail were taken over a range of angles of incidence in steady conditions both in elevation and plan at a tunnel speed of 160 ft/sec. Further photographs throughout the cycle were taken at an incidence of $22{\cdot}2^\circ$ whilst oscillating in heave over a range of frequency parameter, the flash being triggered at the appropriate displacements by an adjustable contact on the forcing mechanism. In each condition at least two photographs were taken in order to establish the repeatability of the measurements. Where the readings did not agree, further photographs were taken until a consistent result was obtained. In analysing the photographs, the position of the centre of the vortex core was assumed to lie on the centre of the smoke tube and this was determined by taking the mean of the positions of the inside edges of the tube relative to the upper surface of the wing (Fig. 5). Most of these measurements were made with a projection microscope giving an image roughly half the model size but, in some cases when the image was faint, the position was estimated directly from the plates with the aid of a magnifying glass and scale.

The diameter of the smoke tube was measured directly from the plates by estimating the difference between the points of maximum smoke intensity (Fig. 5).

In relating the core position to the distance along the centre-line chord some corrections for parallax and perspective errors are required. In the results presented corrections have been applied to reduce errors to a level consistent with the general accuracy of the experiment.

4. *Discussion of Results.*

4.1. *Vortex Core Positions.*

4.1.1. *Static conditions.*—The measurements of the path of the vortex core over a range of wing incidence from 10° to 28° at 160 ft/sec are shown in Fig. 6. The readings taken from the

two plates at each condition are indicated by separate symbols and their general consistency is well established. It has been possible to draw straight lines through the points up to about $0{\cdot}7$ to $0{\cdot}8\ c_0$ but these when produced do not generally pass through the origin and it is suggested that this may be due to interference from the smoke supply and to the camber at the nose. At the lower incidences there is a small upward departure of the points from the straight line at mid-chord and this may be caused by the influence of the main supporting strut. Near the trailing edge the path curves towards the free-stream direction, as would be expected.

The slope of the vortex path relative to the wing surface as indicated by the straight part of the curves in Fig. 6 is plotted against incidence in Fig. 7. This curve indicates that the measurements are very consistent over the whole range of incidence, the maximum scatter being of the order of only $0{\cdot}1°$ in the angle between the core and the wing.

The same points are plotted in Fig. 8 in terms of the vortex height relative to the wing plane ÷ local semi-span $(\partial z/\partial x)\ (1/K)$ against α/K and they are compared with some measurements[4] on a 70° delta wing with a flat upper surface and blunt trailing edge. Considering the differences in wing geometry and measuring techniques, the comparison is satisfactory.

It is clear from Fig. 7 that the height of the vortex core does not vary linearly with incidence and Fig. 9 shows that it varies roughly with $\alpha^{3/4}$. It might be argued that there is more likely to be a simple dependence on the local non-linear contribution to cross-load. Unfortunately the lift distribution has not been measured on this wing and a comparison of this kind cannot be made. However the linear contribution to total lift has been estimated in Fig. 4 and the corresponding non-linear contribution has been found to vary with $\alpha^{3/2}$. Consequently the result of Fig. 9 suggests that the vortex-core height will vary with $\hat{C}_L{}^{1/2}$ though this result may well be particular to the present wing.

The plan positions of the vortex cores were also measured over the same range of incidence but in this case much less consistent results were obtained. In all cases there was a substantial curve in the lines in the mid-chord region due to the influence of the main supporting strut as well as considerable scatter from the mean lines. As many previous measurements of this kind have suggested the plan position of the vortex appears to be far more easily influenced by external disturbances than in elevation.

Taking mean lines through the measured points over the rear half of the wing, the plan position of the cores varied only from $0{\cdot}72$ to $0{\cdot}68$ of the local semi-span through the range of incidence covered (10° to 28°). These results are not sufficiently reliable to be given in detail here but they have been used in the determination of the parallax errors mentioned in Section 3.

4.1.2. *Vortex breakdown.*—Some brief observations of the appearance of the smoke tube when vortex breakdown occurred were made over a range of tunnel speed. Two examples are shown in Fig. 10 in which vortex breakdowns produced at $\alpha = 25°$ and $\beta = 15°$ are photographed with an exposure of about 1 millisecond. The spiral nature of the breakdown previously observed by Lambourne[5] in water-tunnel experiments at low Reynolds numbers is clearly reproduced here at $R_0 = 1{\cdot}5 \times 10^6$ and 6×10^6. Stereoscopic photographs were also obtained and these confirmed the impression that the core spirals in a sense opposite to that of the coiling of the vortex sheet.

4.1.3. *Oscillating conditions.*—The measurements of the path of the vortex core at every 30° through the cycle are given in Figs. 11 and 12 for oscillations in heave at reduced frequencies $(2\pi fc_0/U_0)$ of $3{\cdot}4$ and $1{\cdot}13$ respectively and an incidence of 22°. Straight lines have been drawn through the points up to about $0{\cdot}7\ c_0$ as with the static results. Here again these lines do not pass

through the origin and in some cases appreciable deviations occur, but there are no trends significant enough to be taken into account. Figs. 13 and 14 show the slopes of these lines plotted through the cycle; they are compared with steady values calculated from the effective incidence (taking into account the vertical velocity) and the static values for $\partial z/\partial x$ given in Fig. 7. Fourier analysis of the experimental points gives the following results:

for

$$\frac{2\pi f c_0}{U_0} = 3{\cdot}4$$

$$\frac{\partial z}{\partial x} = \begin{aligned} &0{\cdot}1052 + 0{\cdot}0078 \sin\phi - 0{\cdot}0015 \sin 2\phi + 0 \sin 3\phi - \\ &- 0{\cdot}0135 \cos\phi - 0{\cdot}0012 \cos 2\phi - 0{\cdot}0007 \cos 3\phi \end{aligned}$$

and for

$$\frac{2\pi f c_0}{U_0} = 1{\cdot}13$$

$$\frac{\partial z}{\partial x} = \begin{aligned} &0{\cdot}1043 + 0{\cdot}0033 \sin\phi + 0{\cdot}0002 \sin 2\phi + 0{\cdot}0006 \sin 3\phi - \\ &- 0{\cdot}0042 \cos\phi - 0{\cdot}0005 \cos 2\phi - 0{\cdot}0004 \cos 3\phi \end{aligned}$$

giving a phase lag of the fundamental from the velocity variation of about 60° in the first case and of 51° in the second. It has been assumed in these tests that the smoke tube remains concentric with the vortex core during the oscillatory motion although it is possible that there would be some lag. Consideration of the magnitude of the acceleration of a microscopic smoke particle subjected to an unbalanced viscous drag force suggests, however, that the lag would be very small.

The amplitude of the motion of the vortex core in both cases is greater than the amplitude to be expected from the 'steady' estimates. Fig. 15, which shows the effect of frequency parameter on the core position at points in the cycle when the vertical velocity is zero, suggests that the amplitude may nevertheless remain linear with frequency parameter, since the phase lag is nearly constant.

Some unpublished theoretical works by Randall based on an extension of the Brown and Michael theory gave a phase lag of 28° at a frequency parameter of 1·13 increasing almost linearly to 55° at a frequency parameter of 2. The theory is not expected to be applicable to higher values of frequency parameter.

For the reasons given in Section 4.1.1 the measurements of the plan position of the vortex core on the heaving wing was not satisfactory. The result appeared, however, to confirm Randall's prediction that the movement is small.

A later analysis of these data is given in Appendix II.

4.2. *The Radius of the Smoke Tube.*

Throughout the tests the tubular appearance of the smoke stream was well defined and its radius was observed to vary with incidence, velocity and chordwise distance. The following simple analysis on lines suggested by Maskell shows to what extent the size of the smoke tube indicates the structure of the vortex core.

Consider the forces in the cross-flow plane acting on a single smoke particle when it is in the neighbourhood of the vortex core. Since it is in a rotating flow it will experience a force away from the centre which will be opposed by a drag force arising from the radial velocity of the air and the radial component of the velocity of the particle relative to the vortex core. Forces due to the radial pressure gradient and the radial acceleration of the particle will also occur but it can be shown that these will be negligibly small for the microscopic particles involved. An equilibrium will be reached at a radius from the vortex core where the resultant force in the plane is zero.

In the theory for the outer core of the vortex above a slender wing given by Hall[6], the following expression for the relationship between the three components of velocity is given:

$$\frac{V^2}{U_0^2} = K_1 \left(\frac{U}{U_0} - \frac{W}{U_0} \frac{x}{r} \right)$$

and

$$W \frac{x}{r} = \text{constant}$$

where U_0 is the free-stream velocity,

U, V and W are the axial, circumferential and radial components of velocity respectively,

x is the distance from the wing apex,

r is the radius from the centre of the core,

K_1 is a constant.

The centrifugal force on a smoke particle is given by

$$F_c = \frac{4}{3} \pi r_s^3 \rho_s \frac{V^2}{r}$$

where r_s is the particle radius

and, assuming that Stoke's Law applies, the drag force is given by

$$F_D = 6\pi\mu r_s \left[U \frac{dr}{dx} - W \right]$$

for equilibrium

$$F_c = F_D$$

$$\frac{4}{3} \pi r_s^2 \rho_s \frac{V^2}{r} = 6\pi\mu \left[U \frac{dr}{dx} - W \right]$$

giving, if x is not too small,

$$r^2 = \frac{4}{9} r_s^2 \frac{\rho_s}{\rho_0} R_x K_1 \left\{ \frac{1 - \frac{W}{U} \frac{x}{r}}{1 - 2 \frac{W}{U} \frac{x}{r}} \right\} + C x^{2(W/U)(x/r)} \tag{1}$$

where C is a constant of integration and R_x is the Reynolds number based on distance from the wing apex.

Earnshaw's experimental results given in Ref. 7 show that $(W/U)(x/r)$ may be neglected if r is not much greater than the size of the smoke tube observed in these tests. Thus we have,

$$r^2 = \frac{4}{9} r_s^2 \frac{\rho_s}{\rho_0} K_1 R_x + C \tag{2}$$

Some later unpublished results from Earnshaw suggest K_1 increases roughly linearly with incidence when the latter is not too small. Thus the expression becomes,

$$r^2 = \frac{4}{9} r_s^2 \frac{\rho_s}{\rho_0} R_x K_2 (\alpha - \alpha') + C \tag{3}$$

The approximation introduced by neglecting $(W/U)(x/r)$ implies that the inflow velocity of the air W is small compared with the outflow velocity of the particles near the centre of the core. Further out, however, the force due to the inflow velocity dominates the centrifugal effects and smoke particles originating over a wide area are drawn towards the centre. There is an intermediate

region where the nett inward force is small and a particle will approach the equilibrium position slowly along a spiral path. Smoke observations at much lower speeds (e.g. Fig. 1 in Ref. 2) show that particle paths* make several turns of a spiral before approaching closely to a tubular asymptote, covering an appreciable proportion of the chord in the process. The observed thickness of the 'walls' of the smoke tube may therefore be due partly to the particles spiralling inwards and partly to variation in size. Measurements of smoke-tube radius given here are based on estimated mean thickness of the smoke-tube wall.

Some check on the validity of equation (3) can be made by substituting a value for K_2 from a particular case in Earnshaw's unpublished measurements, corresponding values for r and C from the present work and by assuming that the smoke particles have the same density as water. The resulting value for the radius of the smoke particles is $1{\cdot}2 \times 10^{-5}$ inch. Observation of the colour shift due to the diffraction of transmitted light through the smoke at corresponding conditions suggests a radius of about $0{\cdot}6 \times 10^{-5}$ inch. A measurement in an electron microscope gave a range from $1{\cdot}5$ to 4×10^{-5} inch.

The measurements of the variation of smoke-tube radius with incidence, speed and chordwise distance do not give entirely convincing confirmation of the square-root law indicated in equation (3). In Figs. 16 and 17 the (radius)^2 is shown varying directly with incidence and velocity, although it must be admitted that the same set of measurements could be used just as convincingly to demonstrate linear variations of radius with incidence and velocity. Variation with chordwise distance is particularly sensitive to this difficulty but Fig. 18a suggests that the square-root law may apply over the middle part of the chord.

Fig. 18b shows a roughly linear variation of radius over a distance of two chords from the apex. The observations at the downstream end were difficult to obtain due to slight unsteadiness in the flow but they are sufficiently accurate to indicate a continuous growth of the core downstream of the wing.

To what extent the diameter of the smoke tube gives useful information regarding the structure of the vortex core is not clear. It should be possible from equation (3) to measure the variation of the ratio V^2/U with r by finding the equilibrium radius over a large enough speed range but it would be difficult to make sufficiently accurate measurements of r, r_s and ρ_s. It can be deduced that, where a tube exists, there is a spiral flow of the general type assumed by Hall for the outer core although the distribution of velocities may not be the same. Although the radius of the smoke tube is related to the vortex strength there is no obvious method of deducing in the general case the influence of the vortex on the pressure distribution on the wing surface.

Measurements of the changes in smoke-tube radius during heaving oscillations showed them to be too small to give consistent results.

5. *Conclusions.*

The method of introducing smoke into the outer core of the vortex above a slender wing is capable of giving a clear indication of the path of the core at much higher speed than is usually associated with smoke visualization techniques. It is possible to make accurate measurements of the position of the centre of the core, at least in the steady case.

* It is of interest to note that, according to the preceding analysis, these particle paths differ more from streamlines than is sometimes imagined. For instance, at the equilibrium radius, a particle is subject to a relative velocity equal to $(U\,dr/dx - W)$.

The measurement of the phase lag between the height of the vortex core and the vertical velocity of a wing in a heaving oscillation is not inconsistent with values given by Randall's theoretical work.

Observation of the smoke path in a vortex breakdown at $R_0 = 6 \times 10^6$ confirms the spiral nature of the flow at low Reynolds numbers described by Lambourne[5].

A simple explanation for the tubular appearance of the smoke stream suggests that the radius of this tube is unlikely to provide much information on the structure of the flow field.

6. *Acknowledgement.*

The authors are indebted to Mr. R. N. Wilson of the R.A.E. for the measurement of the radius of the smoke particles with an electron microscope.

SYMBOLS

A	Aspect ratio
C	Constant of integration
c_0	Root chord of wing
C_L	Overall lift coefficient
$\hat{C}_L$	Non-linear contribution to lift coefficient
F_c	Centrifugal force on particle
F_D	Drag force on particle due to radial velocities
f	Frequency of heaving oscillations
K	Cotangent of angle of sweep
K_1 and K_2	Constants
R_0	Reynolds number based on c_0
R_x	Reynolds number based on x
r	Distance of smoke particle from centre of vortex core
r_s	Radius of smoke particle
U	Axial velocity
U_0	Free-stream velocity
V	Circumferential component of velocity
W	Radial component of velocity
x	Distance from wing apex
z	Height normal to wing surface
α	Incidence
β	Angle of sideslip
θ	Angle between vortex core and wing surface
μ	Viscosity of air
ρ_0	Density of air
ρ_s	Density of smoke particle
ϕ	Phase angle from top dead centre

REFERENCES

No.	*Author(s)*	*Title, etc.*
1	H. H. B. M. Thomas	The estimation of stability derivatives (state of the art). A.R.C. C.P.664. A.G.A.R.D. Report 339. August, 1961.
2	R. L. Maltby and R. F. A. Keating	Flow visualization in low-speed wind tunnels: Current British Practice. A.R.C. 22 373. August, 1960.
3	D. Peckham	Low-speed wind-tunnel tests on a series of uncambered slender pointed wings with sharp edges. A.R.C. R. & M. 3186. December, 1958.
4	D. J. Marsden, R. W. Simpson and W. J. Rainbird	An investigation into the flow over delta wings at low speeds with leading edge separations. College of Aeronautics Report 114. A.R.C. 20 409. February, 1958.
5	N. C. Lambourne and D. W. Bryer	The bursting of leading edge vortices—some observations and discussion of the phenomenon. A.R.C. R. & M. 3282. April, 1961.
6	M. G. Hall	A theory for the core of a leading-edge vortex. *J. Fluid Mech.*, Vol. 11, No. 2, pp. 209 to 228. September, 1961.
7	P. B. Earnshaw	An experimental investigation of the structure of a leading-edge vortex. A.R.C. R. & M. 3281. March, 1961.

APPENDIX I

Carbon-Monoxide Poisoning Risks from Smoke

The use of smouldering paper or other cellulose material for flow visualization in wind tunnels introduces an important risk of poisoning from the appreciable carbon-monoxide content of the smoke. The toxic effect is based on the great affinity of haemoglobin in the blood for carbon-monoxide. Very low concentrations in the atmosphere will markedly reduce the capacity of the blood to carry oxygen and the oxygen dissociation rate. The carbon-monoxide can only be displaced slowly by oxygen in a pure atmosphere, so that the effects of breathing a contaminated atmosphere for infrequent short periods over several days are cumulative. The following table gives an indication of the effects of various concentrations.

0·01%	No appreciable effect after prolonged exposure
0·02%	Slight discomfort (e.g. headache) after a few hours exposure
0·15%	Dangerous after 1 hour exposure
0·4%	Fatal after less than 1 hour exposure

The following measurements of carbon-monoxide contamination in the 13 ft × 9 ft Low-Speed Tunnel at R.A.E., Bedford have been made in co-operation with the Department of Propulsion, College of Aeronautics. This tunnel has the unusually large volume of 700 000 cu. ft and concentrations in smaller tunnels might be expected to be correspondingly greater.

CO content of smoke issuing from generator	= 2·5%
CO content of air in working section after burning 6 lb paper	= 0·01%
CO content of air in working section after burning 10 lb paper	= 0·02%
CO concentration in control room at same time	= 0·02%
Short-term local concentrations in the working section up to	0·06%

These figures make it clear that it is necessary to provide good ventilation in the rooms surrounding the tunnel and to maintain a constant circulation of air in the tunnel when attending to the model since there is reason to believe that low chronic toxicity should be avoided as well as the obvious acute poisoning hazard.

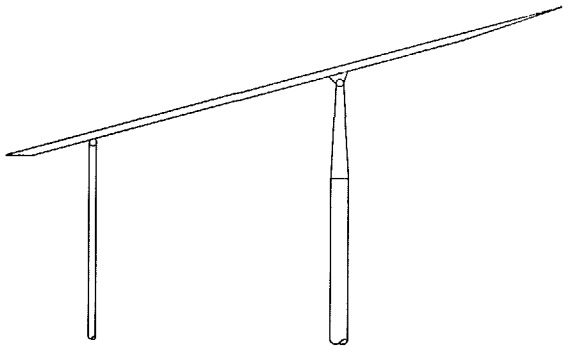

MODEL AND STRUTS.

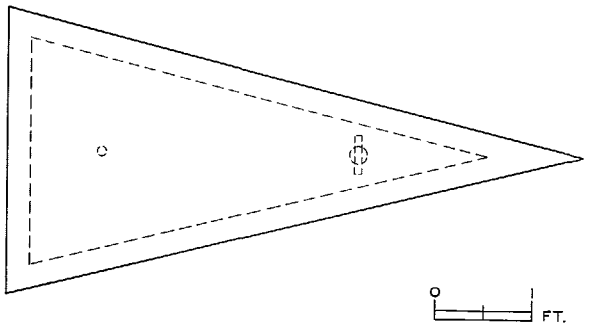

PLANFORM OF MODEL.

FIG. 1. Model details.

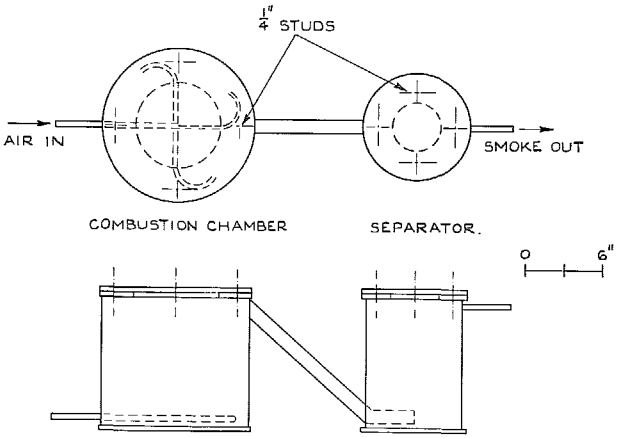

FIG. 2. To. P.S.I. smoke generator.

C

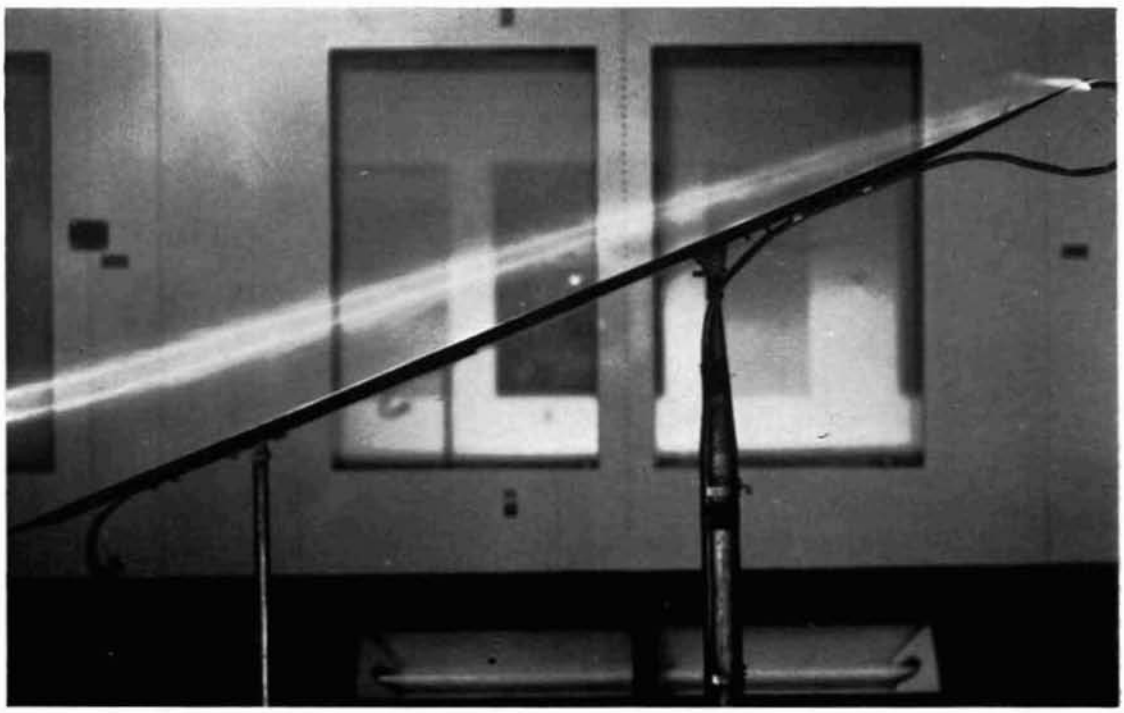

FIG. 3. Arrangement of smoke supply.

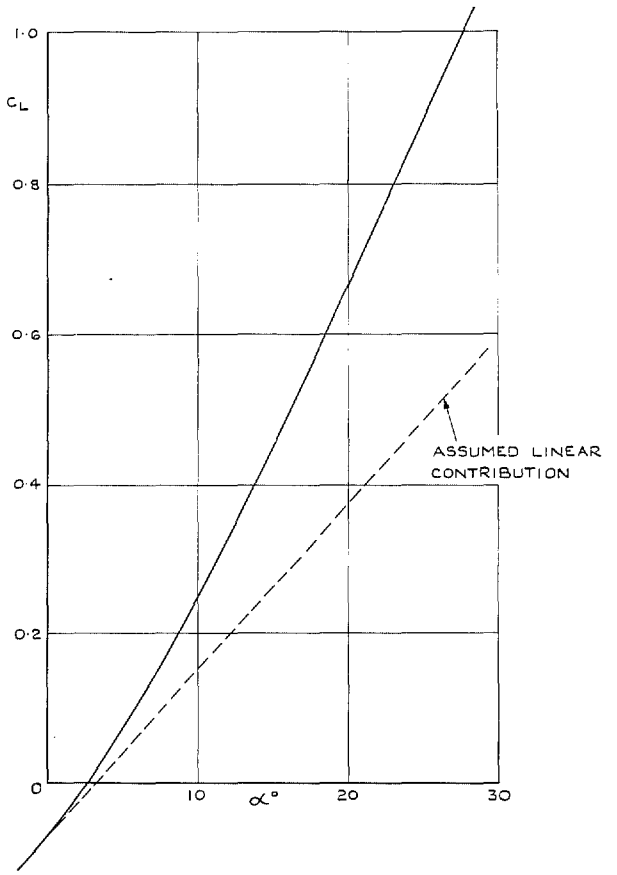

FIG. 4. Lift curve for the wing tested (data from Ref. 3).

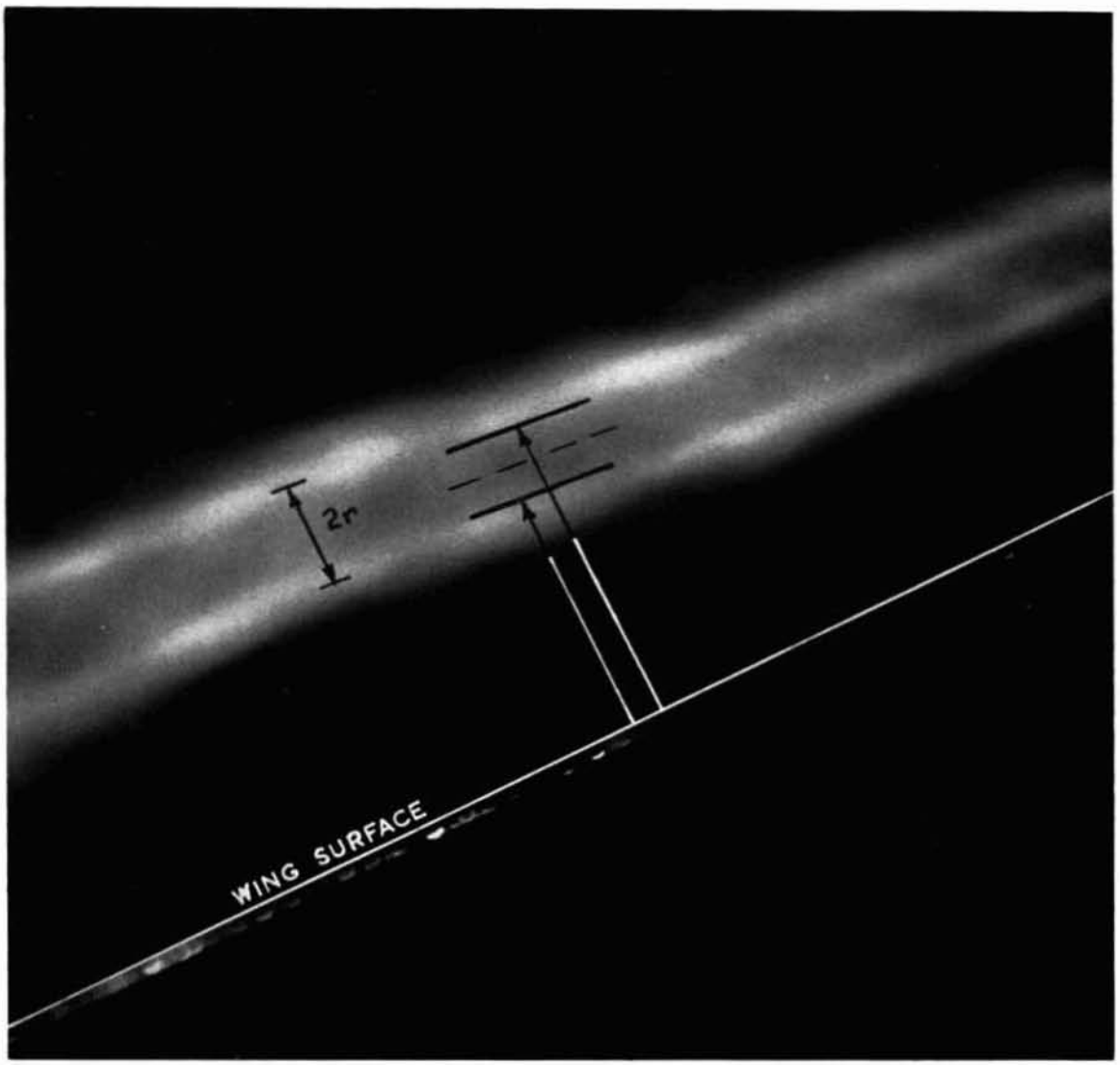

FIG. 5. Measurement of the smoke tube.

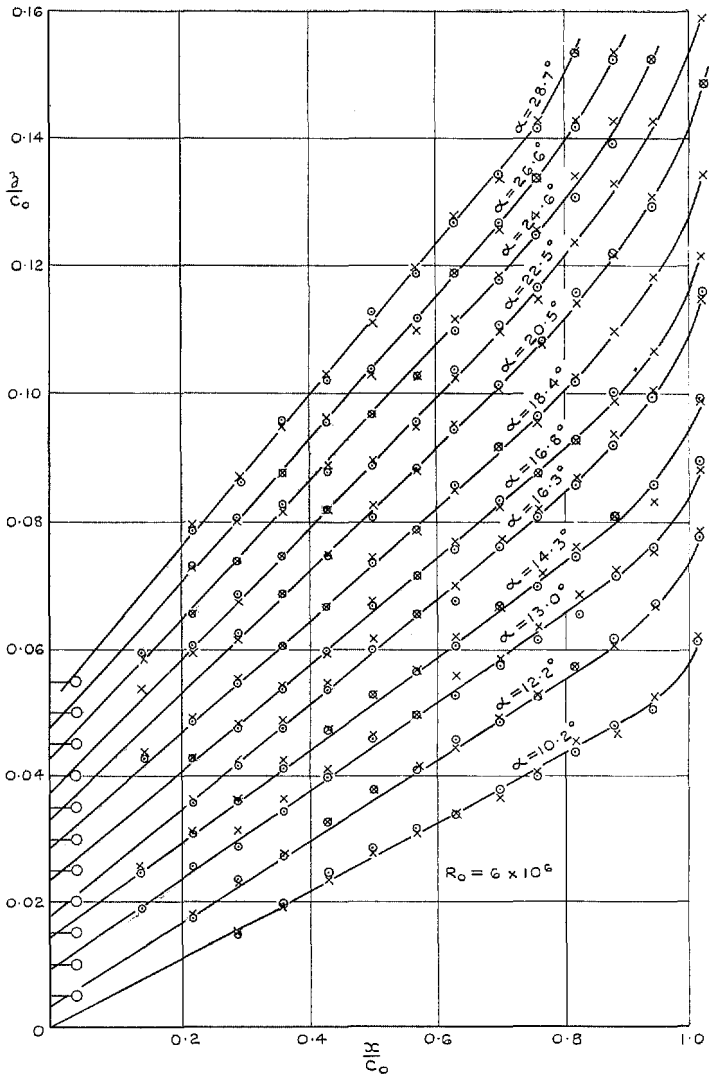

FIG. 6. Variation of height of vortex core along chord (static conditions).

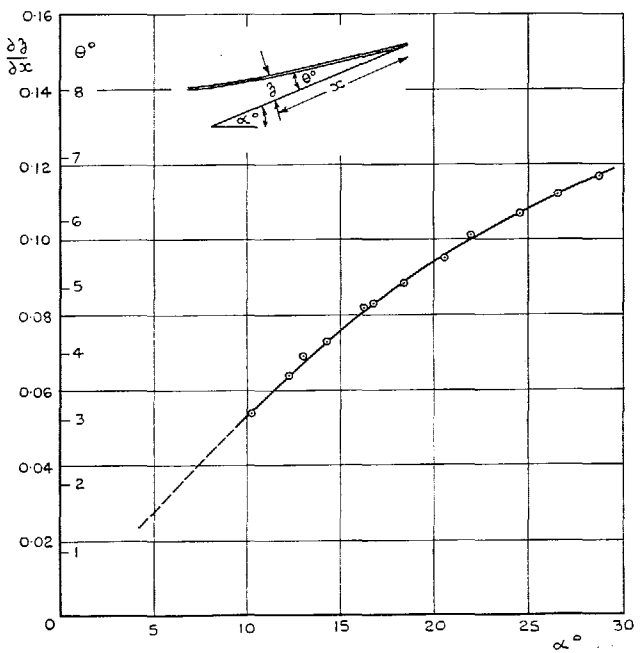

FIG. 7. Slope of vortex core relative to wing surface in static conditions ($R_0 = 6 \times 10^6$).

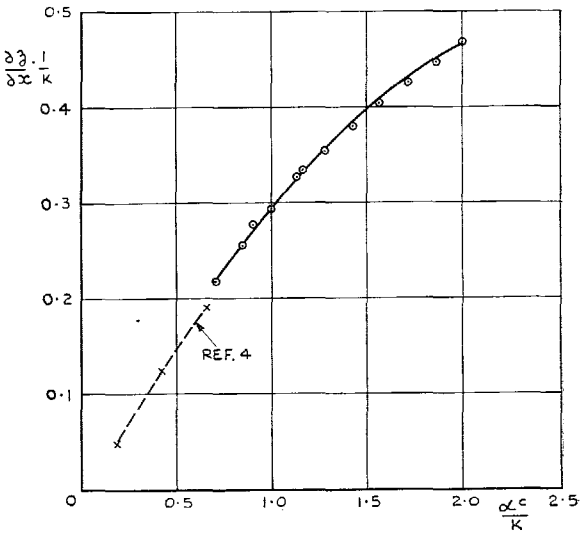

FIG. 8. Slope of vortex core compared with results in Ref. 4.

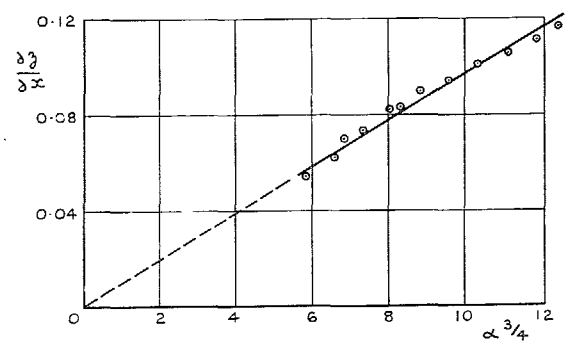

FIG. 9. Slope of vortex core vs. $\alpha^{3/4}$.

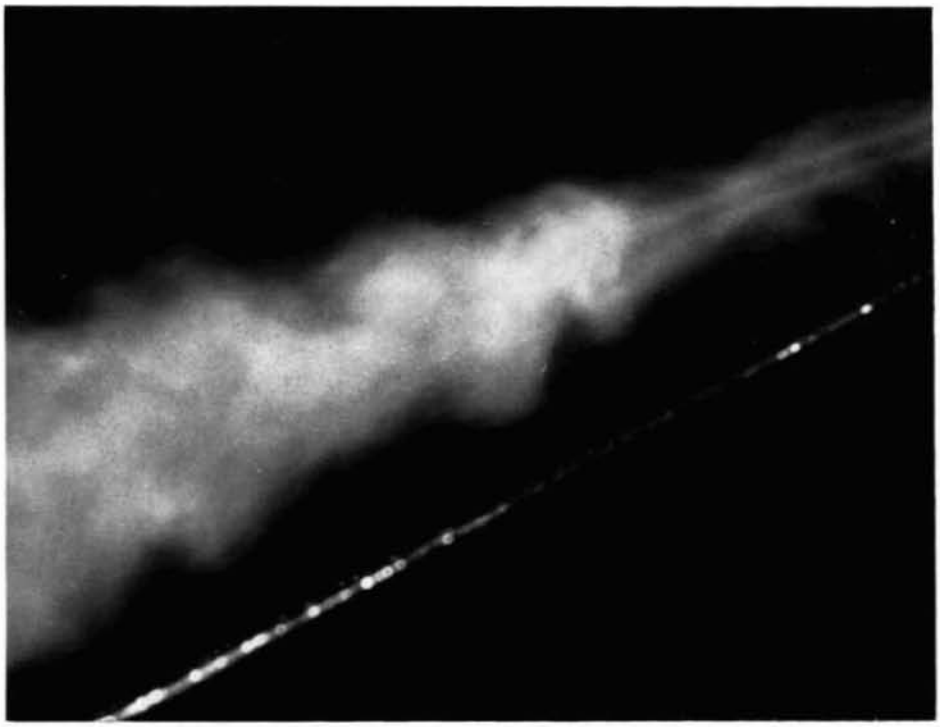

$R_0 = 1{\cdot}5 \times 10^6$

$R_0 = 6 \times 10^6$

FIG. 10. Vortex breakdown.

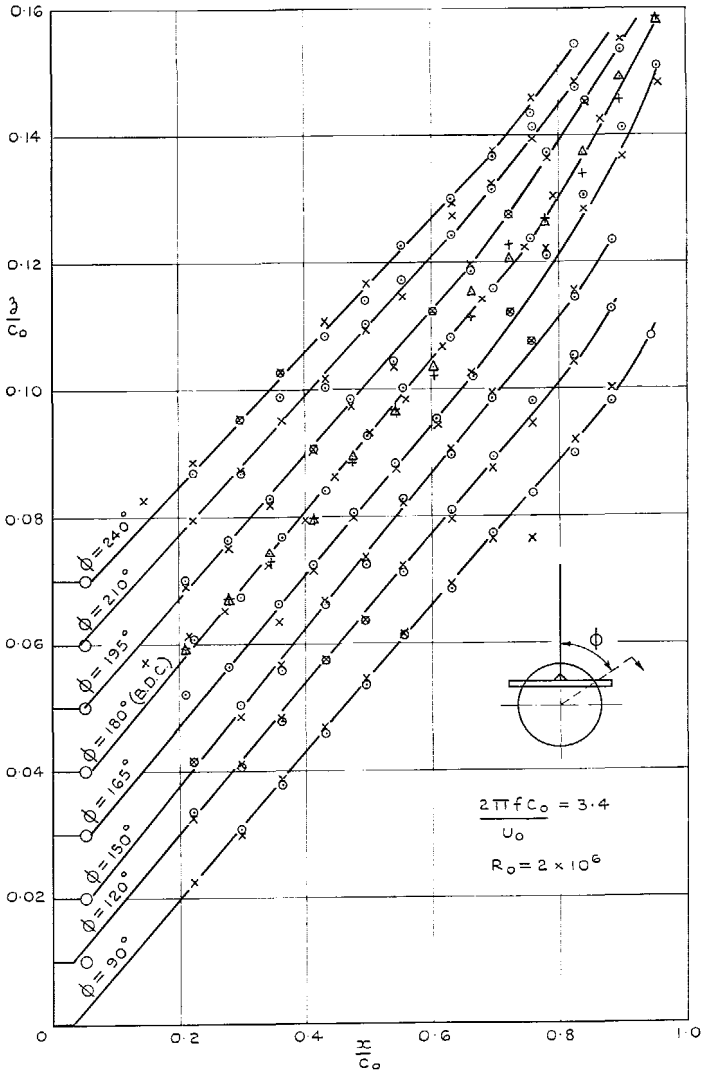

FIG. 11a. Variation of height of vortex core through heaving cycle.

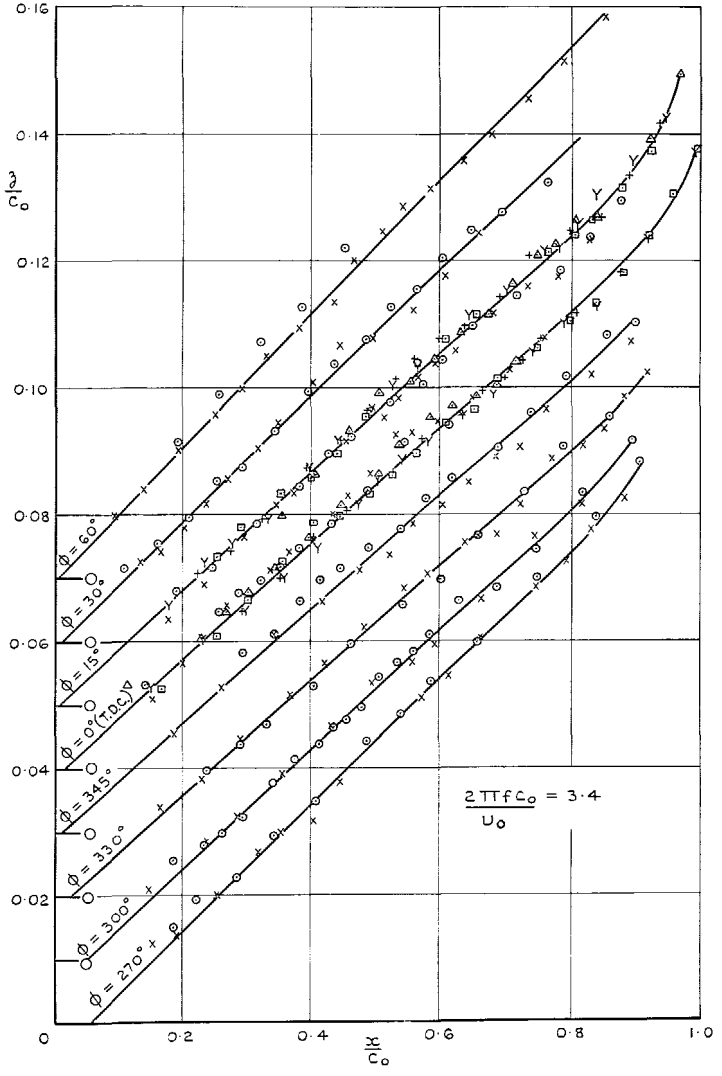

FIG. 11b. Variation of height of vortex core through heaving cycle.

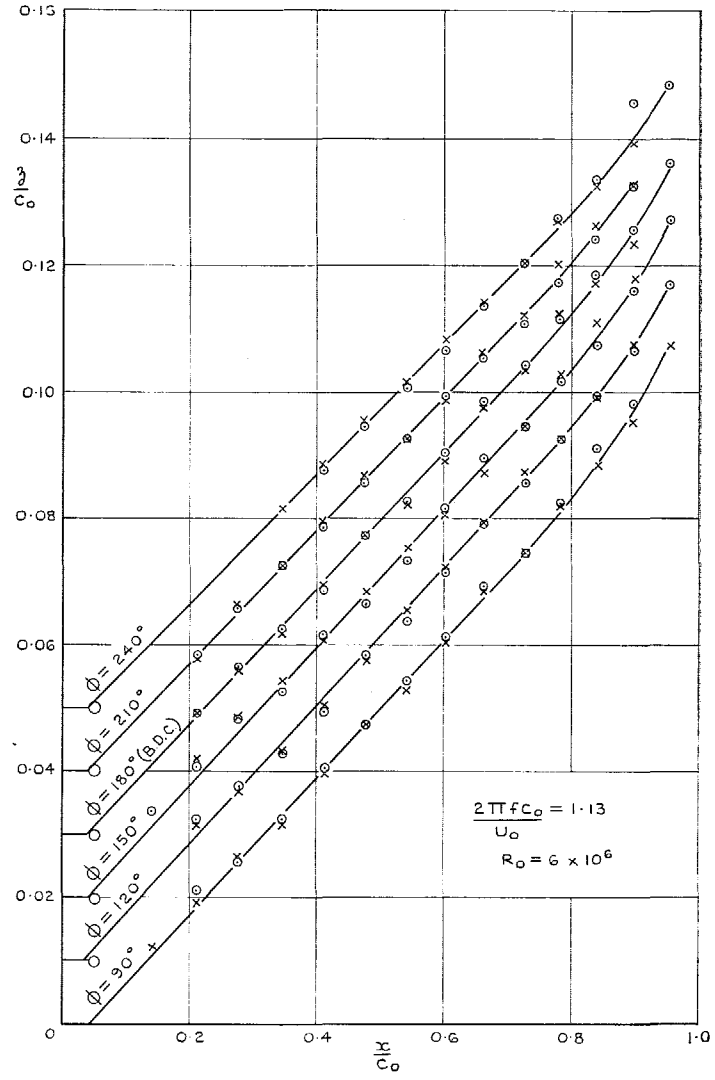

FIG 12a. Variation of height of vortex core through heaving cycle.

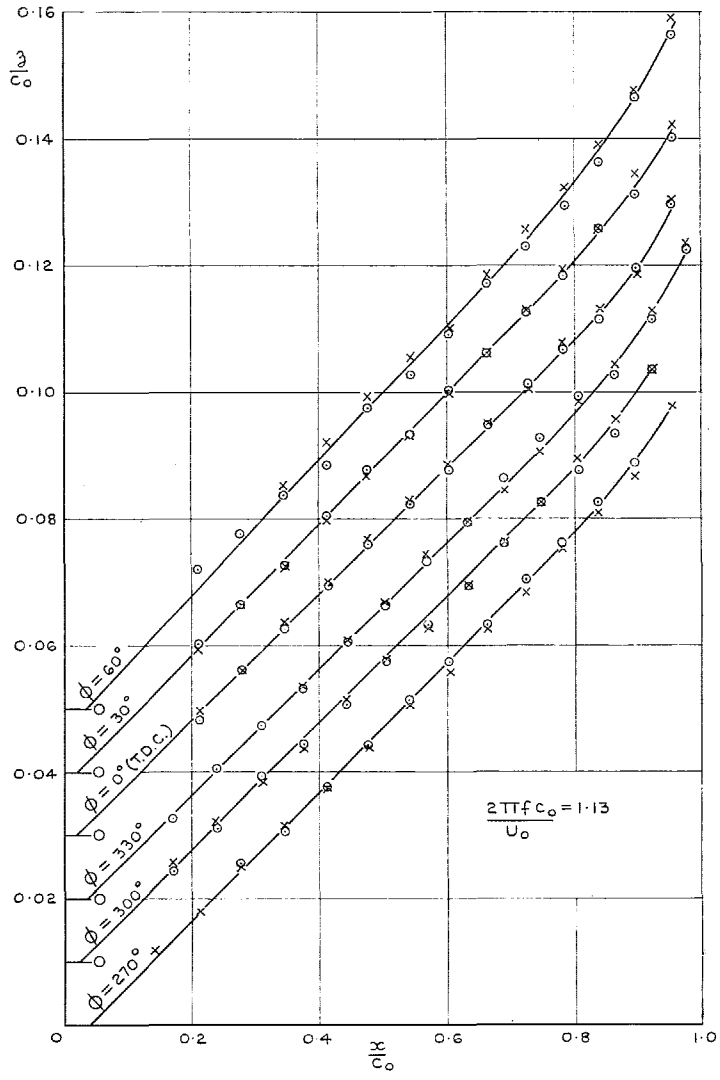

FIG. 12b. Variation of height of vortex core through heaving cycle.

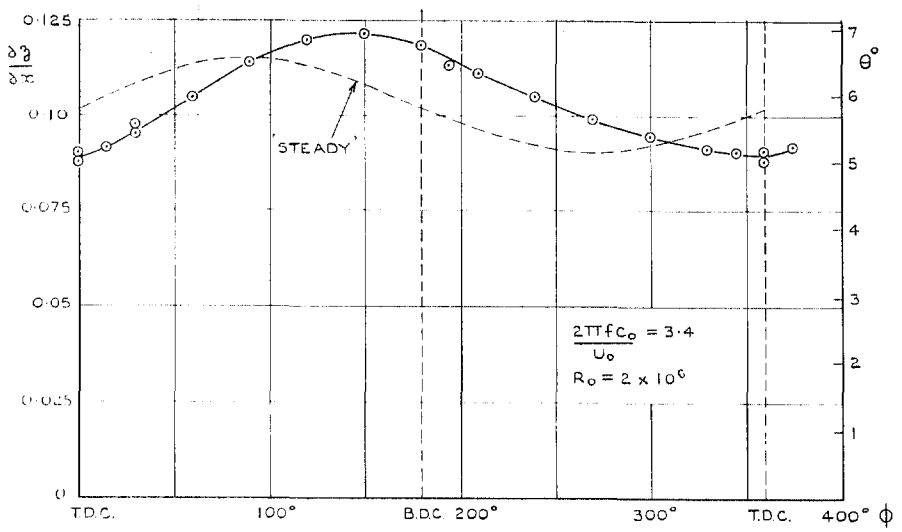

FIG. 13. Variation of vortex height through the cycle ($2\pi fc_0/U_0 = 3{\cdot}4$).

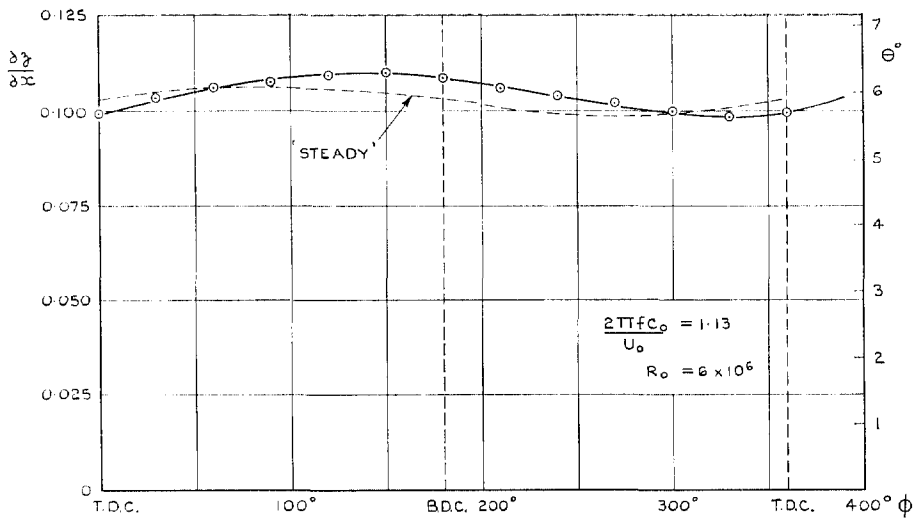

FIG. 14. Variation of vortex height through the cycle ($2\pi fc_0/U_0 = 1{\cdot}13$).

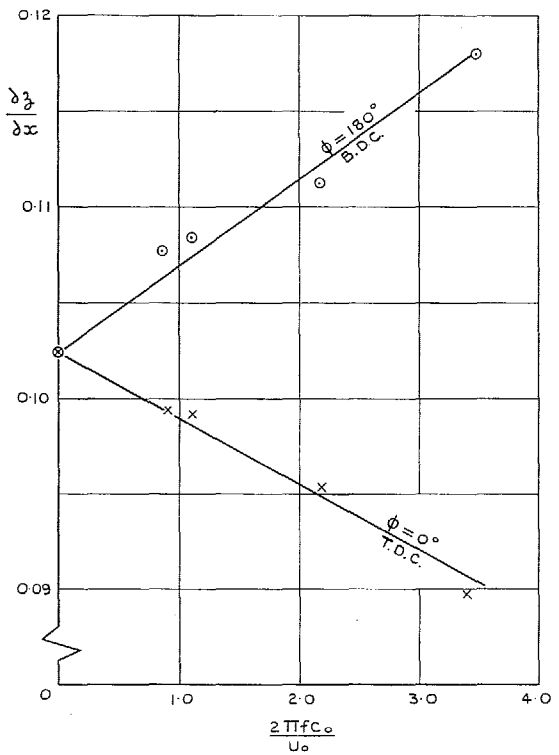

FIG. 15. Variation of vortex height with frequency.

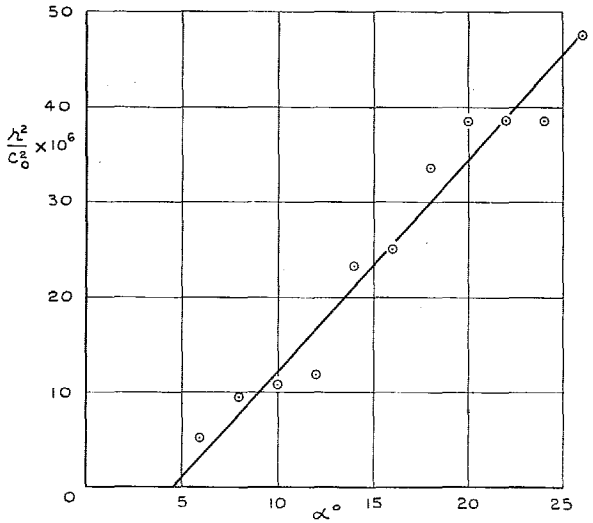

FIG. 16. Variation of smoke-tube radius with incidence ($R_x = 3 \times 10^6$).

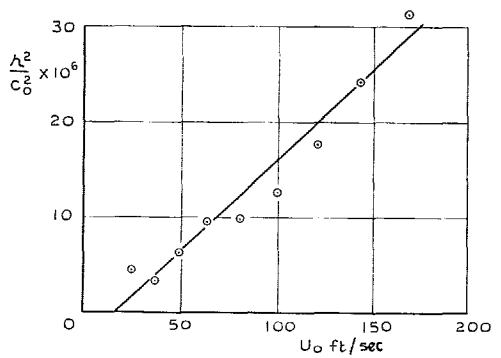

FIG. 17. Variation of smoke-tube radius with speed ($\alpha = 22°$, $x/c_0 = 0{\cdot}5$).

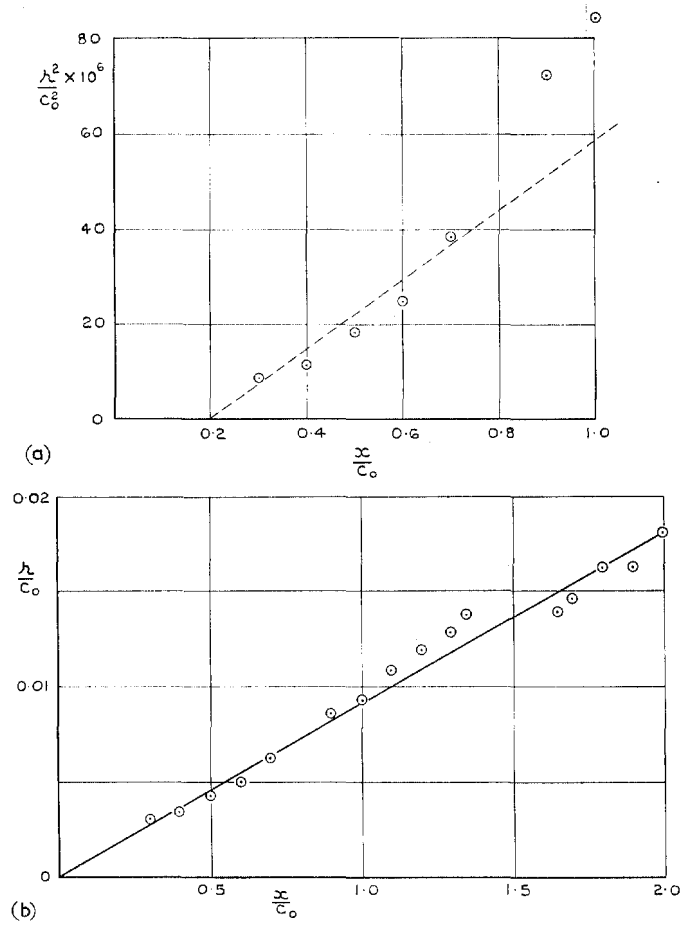

FIG. 18. Variation of smoke-tube radius in chordwise direction ($\alpha = 22°$, $U_0 = 170$ ft/sec).

Addendum

By G. F. Moss

1. *Introduction.*

In the main text Maltby, Engler and Keating describe some low-speed wind tunnel tests in which the height of the leading-edge vortex core was measured on a sharp-edged, aspect ratio 1 delta-wing oscillating in heave. The vortex core was made visible by the introduction of smoke at the apex, and its position above the flat upper wing surface flash-photographed from the side at twelve successive points during the heaving cycle. In the analysis the vortex core above the wing was assumed to be a straight line at each of these twelve cyclic positions and values for the cyclic lag of the core height above the wing with respect to the heaving motion were found accordingly. On reviewing this work, the author felt that at the frequency parameters of the tests (1·85 and 5·55 root chords per cycle) a variation in this cyclic lag along the length of the wing should have been visible. A re-analysis of the raw data was thus made in 1963 and the findings are reported here. In parallel with this, more detailed theoretical calculations were made by the method of Ref. 1 and also, as an independent check on technique, further lag measurements were carried out using a pressure transducer positioned at various points under the vortex.

2. *Method of Analysis.*

The main details of the tunnel tests are given in the main text and need not be repeated here, but the scope of the experiment is shown in the following table:

TABLE 1

Wind speed V ft/sec	50	150
Reynolds Number, R_0	2×10^6	6×10^6
Heaving frequency parameter, $2\pi fc_0/V$	3·40	1·13
Root chords per cycle, V/fc_0	1·85	5·55
Heaving amplitude, z/c_0	$\pm 0{\cdot}021$	$\pm 0{\cdot}021$
Incidence (equivalent), α	$22^\circ \quad \pm 4{\cdot}05^\circ$	$22^\circ \quad \pm 1{\cdot}35^\circ$

In the present analysis, the height of the vortex core above the wing upper surface, measured on the flash photographs, was plotted against crank position at a selected number of positions along the wing root chord. These experimental points are the plotted symbols in Figs. 1 and 2 for the two frequency parameters 1·13 and 3·40 respectively (in the latter case two sets of experimental points were taken). Also plotted in these figures as a dotted line are the corresponding 'steady' vortex heights found by varying incidence by equivalent amounts in a static test.

The best fundamental sine wave was now put through each set of experimental points by means of a Fourier analysis, and this is shown as a full line in Figs. 1 and 2. The following table gives some details of this:

TABLE 2

$\frac{x}{c_0}$	$\frac{z}{c_0}$ Mean Amplitude		Cyclic Lag (degrees)	% Harmonic 2nd	% Harmonic 3rd	% Harmonic 4th	Ratio $\frac{\text{Oscillating Amplitude}}{\text{Steady Amplitude}}$
$2\pi fc_0/V = 1{\cdot}13$							
0·4	0·0381	0·0014	17·9	12·1	35·7	12·1	1·27
0·6	0·0589	0·0027	34·0	8·9	14·4	7·0	1·29
0·8	0·0810	0·0037	35·1	7·3	13·8	2·7	1·37
$2\pi fc_0/V = 3{\cdot}40$							
0·22	0·0199	0·0030	13·4	7·2	8·6	12·0	1·67
0·4	0·0385	0·0052	22·4	2·9	0·7	0·4	1·30
0·6	0·0595	0·0082	41·2	6·6	1·8	2·6	1·28
0·8	0·0812	0·0118	55·0	2·1	5·3	4·7	1·26

In this table, the size of the first few harmonics given by the Fourier analysis is indicated, and this may be regarded as a guide to the accuracy of the experiment in this context. The most reliable experimental data was obtained at the large x/c_0 values at the greater frequency parameter, since the vortex heights were more easily measured and the core more easily seen*. In the last column of Table 2, the ratio of the amplitudes of the z/c_0 waves for the heaving and steady cases is given, and it is shown that there is a considerable increase in the vertical movement of the vortex core in the oscillatory case. In Fig. 3, the steady and oscillatory z/c_0 curves have been compared by 'correcting' for the indicated lag of the latter, and it is clearly seen that this extra movement almost all occurs on the down stroke, or when incidences above the mean value apply. No reason for this 'overshoot' in vortex height is known, but there may well be a significant effect on the forces acting on the wing, and the implied effects on the vortex structure invite further study.

The phase lags at various apex distances, recorded in Table 2, have been plotted in Fig. 4, and approximate curves have been drawn to show the dependence on frequency of the limited amount of data available. The variation along the length of the wing is clearly shown and, for comparison, the values derived from the mean slopes in the previous analysis (in the main text) have been included.

3. *Comparison with Theory.*

The theory of Ref. 1, which uses the Brown and Michael aerodynamic model, gives a variation of phase lag in the height of the vortex core for this wing dependent on the frequency parameter based on the local distance from the apex. In Fig. 5 this is compared with the two sets of experimental data plotted from Table 2, one set ($2\pi fc_0/V = 1{\cdot}13$) showing lag values about 45% greater, and the other set ($2\pi fc_0/V = 3{\cdot}40$) showing lag values about 30% smaller than the theory would predict.

* The smoke was effectively denser at the lower wind speed.

Bearing in mind the experimental difficulties and the assumptions necessary in the theory, the order of agreement is quite encouraging, particularly since the data at the higher values of the frequency parameter $2\pi fx/V$ are really beyond the scope of the theory anyway. However, the (slender) theory indicates a unique relationship between lag and frequency parameter, and at small values of x/c, i.e. well away from the trailing edge, it is difficult to see why the experimental results should not tend to collapse to give one curve also. The possibility that the difference of amplitude between the two sets of data is significant (this is ignored by the theory), or that the model support strut causes interference, cannot be ruled out.

4. *Pressure-Transducer Measurements.*

Some additional phase-lag measurements were obtained by comparing a signal in-phase with the motion of the model, produced by a magslip geared to the drive, with the signal from a flush-mounted pressure transducer (Ref. 2) on the wing upper surface. The comparison was made using a Muirhead Phase Meter. A series of positions for the pressure transducer were used, all lying along a line through the apex at 2/3 semi-span. The reference side of the transducer was connected to a point on the centre-line chord on the wing upper surface at 60% c_0, at which point only comparatively small variations of pressure occurred* (of the order of 20% of those under the vortex core).

The comparison of these pressure phase-lag results with the phase lags found previously in the height variation of the vortex, are shown in Fig. 6. Only pressure measurements at the lower frequency parameter, $2\pi fc_0/V = 1{\cdot}13$, were possible because of a sensitivity limitation of the transducer but the comparison shows clearly the good measure of agreement between the two sets of results. It should be borne in mind, however, that the variation of pressure at the transducer through the heaving cycle will be affected by the variation of vortex strength as well as by the height of the vortex above the surface.

5. *Conclusions.*

A re-analysis of the experimental data has shown that a much better agreement with theory (Ref. 1) is established when the vortex cores above the wing are not assumed to be straight. The associated variation of phase lag in vortex height with distance from the apex has been confirmed by further experimental work using pressure transducers. The overall conclusion is that the large phase lags predicted by theory for an oscillating slender wing, full scale, are substantiated by this experimental work.

REFERENCES

No.	*Author(s)*	*Title, etc.*
1	D. G. Randall	A Theoretical Determination of the Flow Past and the Air Forces on an Oscillating Slender Delta Wing with Leading Edge Separation. R.A.E. Report Structures 284. A.R.C. 24 910. March, 1963.
2	W. R. MacDonald and P. W. Cole	A Sub-Miniature Differential Pressure Transducer for use in Wind Tunnel Models. R.A.E. Tech. Note Instn. 169. January, 1961.

* Prior attempts to use an independent reference pressure for the transducer all failed owing to acceleration effects in pressure leads.

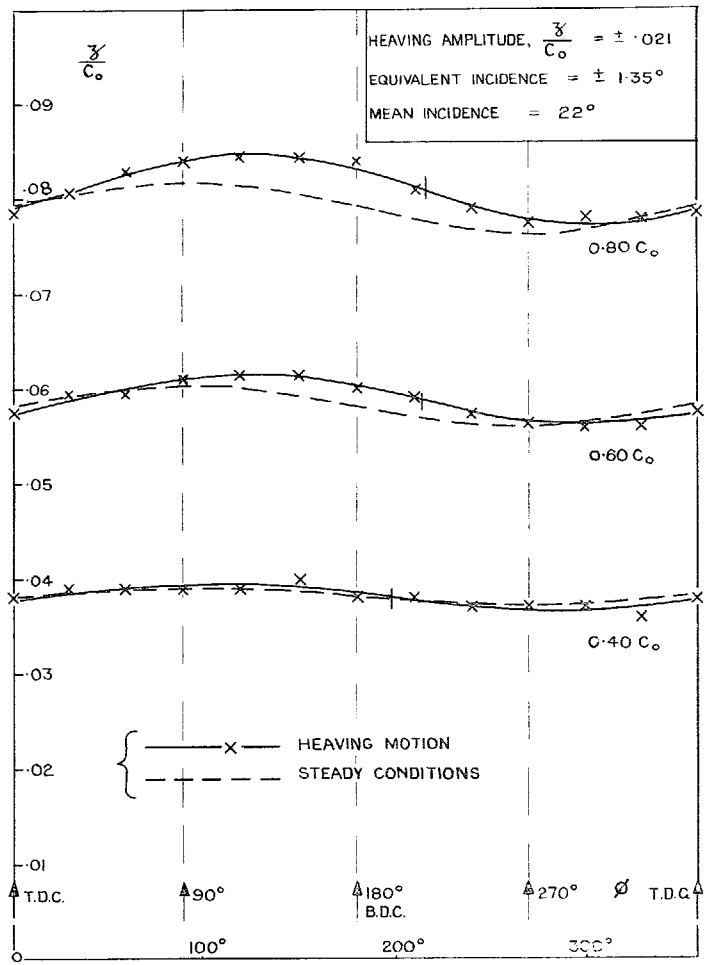

FIG. 1. Cyclic variation of vortex height: $R_0 = 6 \times 10^6$, $2\pi f c_0/V = 1{\cdot}13$.

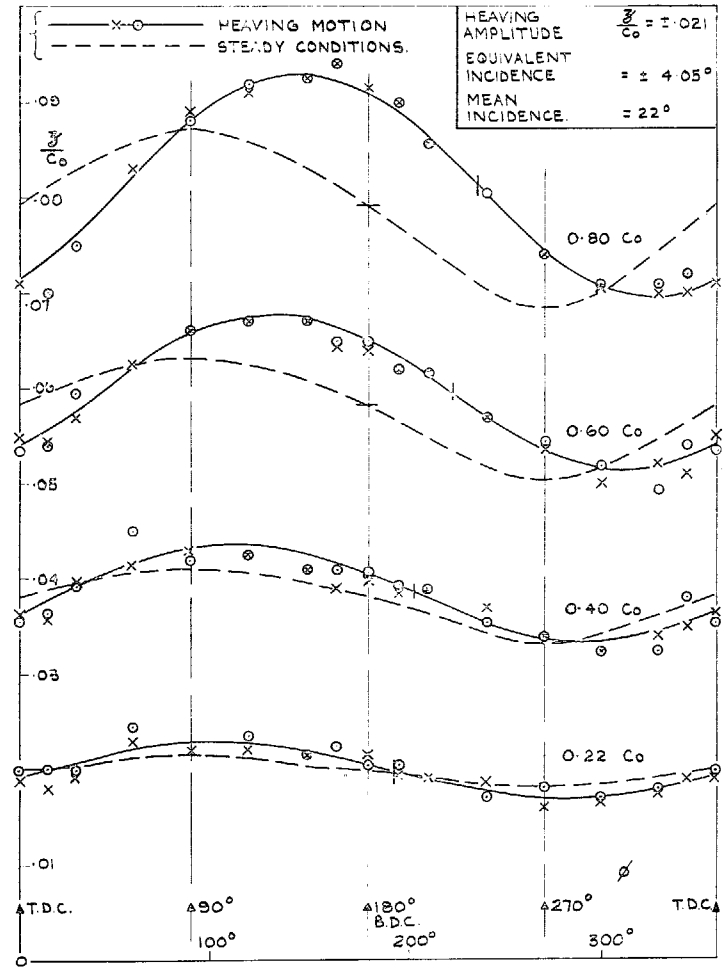

FIG. 2. Cyclic variation of vortex height: $R_0 = 2 \times 10^6$, $2\pi f c_0/V = 3{\cdot}4$.

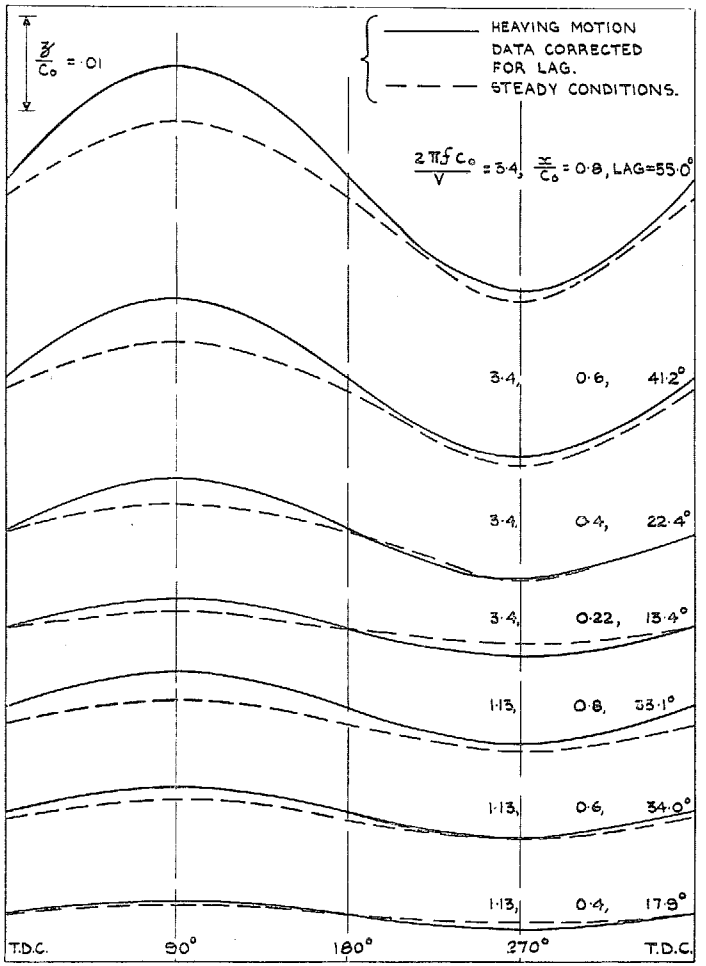

FIG. 3. Amplitude of vortex height, steady and heaving.

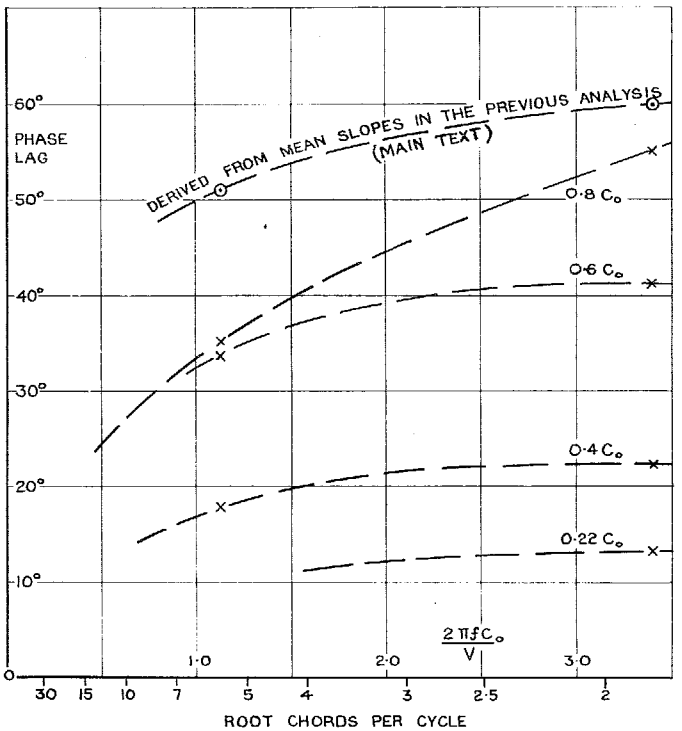

FIG. 4. Mean cyclic height of vortex-height variation with frequency.

(91657) Wt. 67/3301 K5 7/65 Hw.

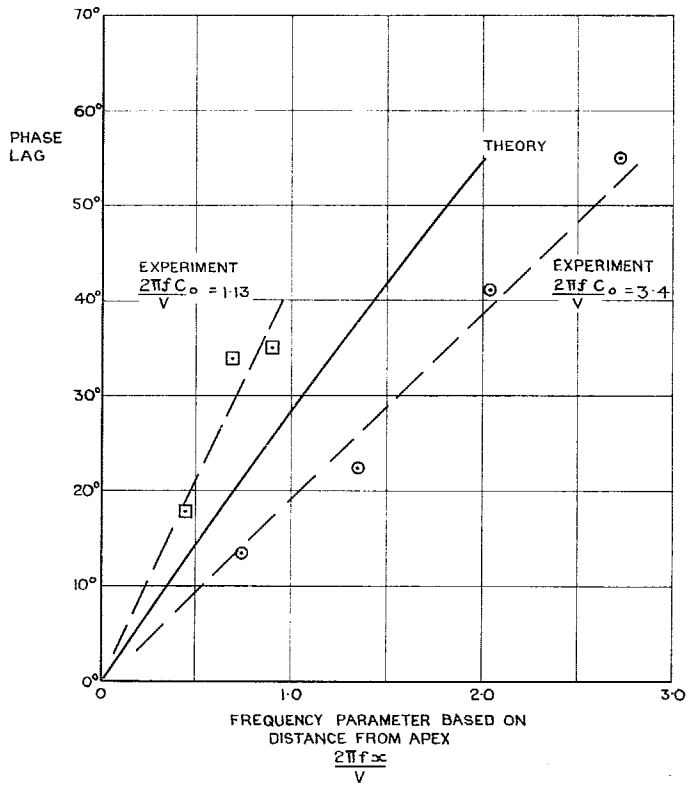

FIG. 5. Mean cyclic lag of vortex height: variation with local frequency parameter.

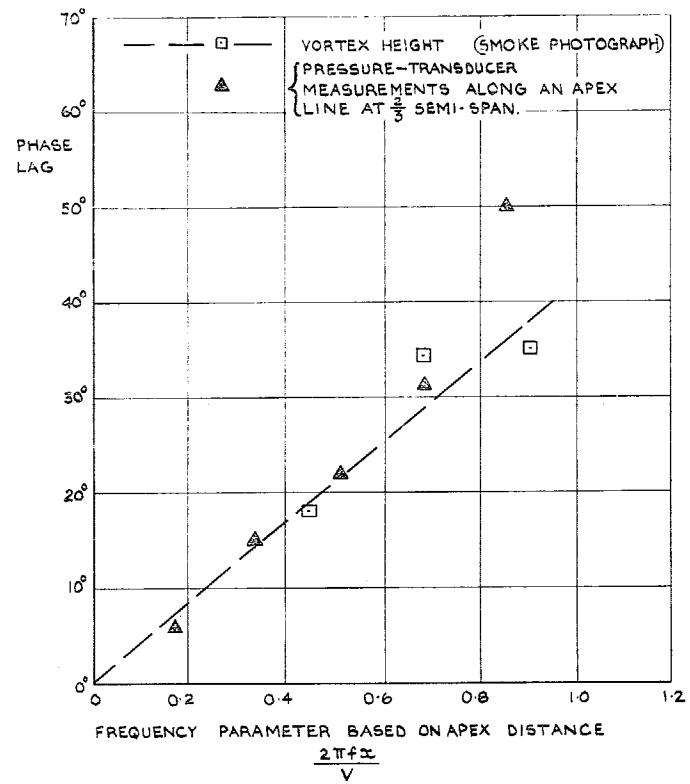

FIG. 6. Comparison of measured lag.

Publications of the Aeronautical Research Council

ANNUAL TECHNICAL REPORTS OF THE AERONAUTICAL RESEARCH COUNCIL (BOUND VOLUMES)

1945 Vol. I. Aero and Hydrodynamics, Aerofoils. £6 10*s*. (£6 13*s*. 6*d*.)
Vol. II. Aircraft, Airscrews, Controls. £6 10*s*. (£6 13*s*. 6*d*.)
Vol. III. Flutter and Vibration, Instruments, Miscellaneous, Parachutes, Plates and Panels, Propulsion. £6 10*s*. (£6 13*s*. 6*d*.)
Vol. IV. Stability, Structures, Wind Tunnels, Wind Tunnel Technique. £6 10*s*. (£6 13*s*. 3*d*.)

1946 Vol. I. Accidents, Aerodynamics, Aerofoils and Hydrofoils. £8 8*s*. (£8 11*s*. 9*d*.)
Vol. II. Airscrews, Cabin Cooling, Chemical Hazards, Controls, Flames, Flutter, Helicopters, Instruments and Instrumentation, Interference, Jets, Miscellaneous, Parachutes. £8 8*s*. (£8 11*s*. 3*d*.)
Vol. III. Performance, Propulsion, Seaplanes, Stability, Structures, Wind Tunnels. £8 8*s*. (£8 11*s*. 6*d*.)

1947 Vol. I. Aerodynamics, Aerofoils, Aircraft. £8 8*s*. (£8 11*s*. 9*d*.)
Vol. II. Airscrews and Rotors, Controls, Flutter, Materials, Miscellaneous, Parachutes, Propulsion, Seaplanes, Stability, Structures, Take-off and Landing. £8 8*s*. (£8 11*s*. 9*d*.)

1948 Vol. I. Aerodynamics, Aerofoils, Aircraft, Airscrews, Controls, Flutter and Vibration, Helicopters, Instruments, Propulsion, Seaplane, Stability, Structures, Wind Tunnels. £6 10*s*. (£6 13*s*. 3*d*.)
Vol. II. Aerodynamics, Aerofoils, Aircraft, Airscrews, Controls, Flutter and Vibration, Helicopters, Instruments, Propulsion, Seaplane, Stability, Structures, Wind Tunnels. £5 10*s*. (£5 13*s*. 3*d*.)

1949 Vol. I. Aerodynamics, Aerofoils. £5 10*s*. (£5 13*s*. 3*d*.)
Vol. II. Aircraft, Controls, Flutter and Vibration, Helicopters, Instruments, Materials, Seaplanes, Structures, Wind Tunnels. £5 10*s*. (£5 13*s*.)

1950 Vol. I. Aerodynamics, Aerofoils, Aircraft. £5 12*s*. 6*d*. (£5 16*s*.)
Vol. II. Apparatus, Flutter and Vibration, Meteorology, Panels, Performance, Rotorcraft, Seaplanes. £4 (£4 3*s*.)
Vol. III. Stability and Control, Structures, Thermodynamics, Visual Aids, Wind Tunnels. £4 (£4 2*s*. 9*d*.)

1951 Vol. I. Aerodynamics, Aerofoils. £6 10*s*. (£6 13*s*. 3*d*.)
Vol. II. Compressors and Turbines, Flutter, Instruments, Mathematics, Ropes, Rotorcraft, Stability and Control, Structures, Wind Tunnels. £5 10*s*. (£5 13*s*. 3*d*.)

1952 Vol. I. Aerodynamics, Aerofoils. £8 8*s*. (£8 11*s*. 3*d*.)
Vol. II. Aircraft, Bodies, Compressors, Controls, Equipment, Flutter and Oscillation, Rotorcraft, Seaplanes, Structures. £5 10*s*. (£5 13*s*.)

1953 Vol. I. Aerodynamics, Aerofoils and Wings, Aircraft, Compressors and Turbines, Controls. £6 (£6 3*s*. 3*d*.)
Vol. II. Flutter and Oscillation, Gusts, Helicopters, Performance, Seaplanes, Stability, Structures, Thermodynamics, Turbulence. £5 5*s*. (£5 8*s*. 3*d*.)

1954 Aero and Hydrodynamics, Aerofoils, Arrester gear, Compressors and Turbines, Flutter, Materials, Performance, Rotorcraft, Stability and Control, Structures. £7 7*s*. (£7 10*s*. 6*d*.)

Special Volumes

Vol. I. Aero and Hydrodynamics, Aerofoils, Controls, Flutter, Kites, Parachutes, Performance, Propulsion, Stability. £6 6*s*. (£6 9*s*.)
Vol. II. Aero and Hydrodynamics, Aerofoils, Airscrews, Controls, Flutter, Materials, Miscellaneous, Parachutes, Propulsion, Stability, Structures. £7 7*s*. (£7 10*s*.)
Vol. III. Aero and Hydrodynamics, Aerofoils, Airscrews, Controls, Flutter, Kites, Miscellaneous, Parachutes, Propulsion, Seaplanes, Stability, Structures, Test Equipment. £9 9*s*. (£9 12*s*. 9*d*.)

Reviews of the Aeronautical Research Council

1949–54 5*s*. (5*s*. 5*d*.)

Index to all Reports and Memoranda published in the Annual Technical Reports

1909–1947 R. & M. 2600 (out of print)

Indexes to the Reports and Memoranda of the Aeronautical Research Council

Between Nos. 2451–2549: R. & M. No. 2550 2*s*. 6*d*. (2*s*. 9*d*.); Between Nos. 2651–2749: R. & M. No. 2750 2*s*. 6*d*. (2*s*. 9*d*.); Between Nos. 2751–2849: R. & M. No. 2850 2*s*. 6*d*. (2*s*. 9*d*.); Between Nos. 2851–2949: R. & M. No. 2950 3*s*. (3*s*. 3*d*.); Between Nos. 2951–3049: R. & M. No. 3050 3*s*. 6*d*. (3*s*. 9*d*.); Between Nos. 3051–3149: R. & M. No. 3150 3*s*. 6*d*. (3*s*. 9*d*.); Between Nos. 3151–3249: R. & M. No. 3250 3*s*. 6*d*. (3*s*. 9*d*.); Between Nos. 3251–3349: R. & M. No. 3350 3*s*. 6*d*. (3*s*. 10*d*.)

Prices in brackets include postage

Government publications can be purchased over the counter or by post from the Government Bookshops in London, Edinburgh, Cardiff, Belfast, Manchester, Birmingham and Bristol, or through any bookseller

Printed and published by
HER MAJESTY'S STATIONERY OFFICE

To be purchased from
York House, Kingsway, London W.C.2
423 Oxford Street, London W.1
13A Castle Street, Edinburgh 2
109 St. Mary Street, Cardiff
39 King Street, Manchester 2
50 Fairfax Street, Bristol 1
35 Smallbrook, Ringway, Birmingham 5
80 Chichester Street, Belfast 1
or through any bookseller

Printed in England

R. & M. No. 3410

S.O. Code No. 23-3410